sustainability

MDPI

Article

Development of Artificial Stone through the Recycling of Construction and Demolition Waste in a Polymeric Matrix

Marcelo Barcellos Reis [1,*], Henry Alonso Colorado Lopera [1,2], Carlos Maurício Fontes Vieira [1], Afonso Rangel Garcez Azevedo [3], Elaine Aparecida Santos Carvalho [1] and Sérgio Neves Monteiro [4]

[1] Advanced Materials Laboratory (LAMAV), State University of Norte Fluminense-UENF, Av. Alberto Lamego 2000, Campos dos Goytacazes 28013-602, RJ, Brazil; henry.colorado@udea.edu.co (H.A.C.L.); vieira@uenf.br (C.M.F.V.); elainesanttos@yahoo.com.br (E.A.S.C.)
[2] CCComposites Laboratory, University of Antioquia (UdeA), Medellín 050010, Colombia
[3] Civil Engineering Laboratory (LECIV), State University of Norte Fluminense-UENF, Av. Alberto Lamego 2000, Campos dos Goytacazes 28013-602, RJ, Brazil; afonso@uenf.br
[4] Department of Materials Science, Military Institute of Engineering (IME), Praça General Tibúrcio 80, Praia Vermelha, Urca, Rio de Janeiro 22290-270, RJ, Brazil; snevesmonteiro@gmail.com
* Correspondence: mbarcellosreis@gmail.com

Abstract: Civil construction is one of the oldest activities known to humanity, with reports indicating that builders from the Roman Empire were already seeking to reuse materials. Currently, considering the depletion of natural resource supplies, the recycling of solid construction and demolition waste (CDW) not only provides new products but also presents ecological and economical alternatives. In this context, this research explores new variables for the disposal of CDW, with the manufacturing of artificial finishing stones appearing as a strong possibility to be studied. This research presents the development of a new composite from CDW, using an orthophthalic polyester resin as a binder. The waste was sieved and separated by granulometry using the simplex centroid method. The best-compacted mixture was determined statistically by ANOVA and Tukey's test. The waste was characterized by X-ray fluorescence, and the resin by Fourier transform infrared spectroscopy. Artificial stone slabs were produced with 85% waste and 15% resin by mass, using the vibro-compression and vacuum system. They were subsequently cut for mechanical, physical, and chemical tests. Microstructural analysis was performed using scanning electron microscopy on the surfaces of the fractured compositions, as well as on the grains. The artificial stone with the best results had a density of 2.256 g/cm^3, a water absorption of 0.69%, and an apparent porosity of 1.55%. It also exhibited a flexural strength of 34.74 MPa and a compressive strength of 111.96 MPa, alongside good results in alterability and thermal tests. In this satisfactory scenario, the use of this waste in the composition of artificial stones is promising, as it directly aligns with the concept of sustainable development. It replaces the end-of-life concept of the linear economy with new circular flows of reuse, restoration, and renewal, in an integrated process of the circular economy. Additionally, the quality of the final product exhibits properties similar to those of commercially available artificial stones.

Keywords: construction waste; artificial rock; polyester resin; environment

check for updates

Citation: Reis, M.B.; Colorado Lopera, H.A.; Vieira, C.M.F.; Azevedo, A.R.G.; Carvalho, E.A.S.; Monteiro, S.N. Development of Artificial Stone through the Recycling of Construction and Demolition Waste in a Polymeric Matrix. *Sustainability* **2024**, *16*, 5952. https://doi.org/10.3390/su16145952

Academic Editors: Andrzej Pacana and Dominika Siwiec

Received: 4 June 2024
Revised: 4 July 2024
Accepted: 9 July 2024
Published: 12 July 2024

Copyright: © 2024 by the authors. Licensee MDPI, Basel, Switzerland. This article is an open access article distributed under the terms and conditions of the Creative Commons Attribution (CC BY) license (https://creativecommons.org/licenses/by/4.0/).

1. Introduction

Construction is one of the oldest activities known to humanity. The production and application of concrete for use in buildings is present all over the planet, regardless of the economic and geographical conditions of each country, with Portland cement being the second most consumed material in the world, second only to water [1]. Thus, considering its high consumption, research has been conducted for many years to evaluate the various conditions of technological performance [2], durability [3], potential for the application of new materials [4], and issues related to its sustainability [5] materials, such as concrete

and mortars. Construction and demolition waste is one of the main sources of recycled aggregate production worldwide, due to its high availability and compatibility [6,7].

Currently, the focus on environmental preservation has intensified the reuse of solid waste in civil construction, requiring regulations to support and guide proper disposal and reuse procedures. It is estimated that civil construction consumes between 14% and 50% of the natural resources available on the planet [8].

Numerous studies have been conducted to evaluate the use of recycled aggregates in civil construction. There is a consensus in the scientific community that the generation of construction and demolition waste is considered an unsustainable activity, as it causes constant environmental degradation. It is estimated that up to 48% of the total urban solid waste generated globally comes from civil construction [9]. In Brazil, for example, construction companies are responsible for 52% of the construction waste generated, while the remainder is generated informally. Additionally, due to their bulky and high-density nature, the disposal of these wastes creates a significant and irreversible environmental impact [10]. The use of this waste is an important tool in combating environmental degradation, both directly and indirectly, by reducing the consumption of construction materials derived from the crushing of stones, gravel, and artificial sand. Additionally, recycling not only adds value to the final product but also reintegrates a material that would otherwise remain discarded in landfills for many years. In developing countries, this waste often ends up in unstructured dumpsites.

Research indicates optimization in the mechanical properties of various materials using recycled aggregate, such as increased mechanical strength [11].

On the other hand, the type of recycled aggregate affects the performance of materials differently. Thus, highlighted an increase in impact resistance when recycled coarse aggregates were used in concrete blocks. They also pointed out that the incorporation of recycled fine aggregates from construction and demolition waste can increase the mechanical strength of concrete due to the particles of non-hydrated cement in the recycled material, remembering that the loss of mechanical strength is a limiting factor for the use of recycled aggregates and is greater when the water/cement ratio is lower. Notwithstanding the above, some authors justified the increase in compressive strength in concretes with recycled fine aggregates due to the pozzolanic effect of fine particles.

The higher fine content in recycled aggregates can improve the transition zone between the cement matrix and the aggregate, contributing to greater concrete compaction. According to [12], fine particles provide better packing. Since recycled aggregate has higher absorption, it promotes better adhesion between the cement paste and the aggregate through the absorption of the paste and the precipitation of hydration crystals in the aggregate's pores. The presence of old mortar particles adhered to the grains of recycled aggregate is a significant characteristic that affects the behavior of the concrete. This presence can correlate with higher water absorption, increased porosity, and a lower strength of recycled concrete [13].

The use of recycled aggregates in paving is the most accepted alternative in the technical field [14]. The simplest form of recycling is the application of debris in the form of current gravel, in bases, sub-bases, and primary paving layers. Using construction and demolition waste in base, sub-base, and primary layers offers numerous advantages and significantly lowers construction costs compared to those produced with graded gravel or soil additives [15].

In parallel, artificial stones are innovative materials manufactured with a polymeric resin and a high percentage of natural aggregates, which can be partially replaced by waste. The mechanical properties of artificial stone surpass those of natural stones, as the use of resin in its production results in a less porous material with a lower water absorption rate and better mechanical strength, making them suitable for more demanding applications, such as flooring and wall coverings [16,17].

Artificial stone is highly attractive for domestic environments due to its variety and consistency of colors, and resistance to scratches, chips, and stains. The popularity of

artificial stone has rapidly increased worldwide. Analyzing the Brazilian ornamental stone market, ABIROCHAS [18] shows that imports of artificial stones are twice as high as imports of natural stones, as shown in Figure 1. The cumulative imports of artificial stones over the past ten years have seen an increase of nearly 120%, highlighting its emerging market and emphasizing the importance of research in this area for the development of new materials for the Brazilian market.

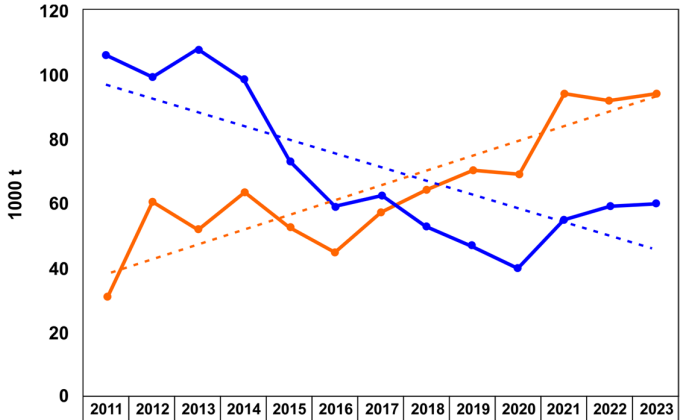

	2011	2012	2013	2014	2015	2016	2017	2018	2019	2020	2021	2022	2023
Natural Rocks	106	99	108	98	73	59	63	53	47	40	55	59	60
Artificial Rocks	31	60	52	63	53	45	57	64	70	69	94	92	94

Figure 1. Demonstration of the evolution of imports of rocks (period of 2011 to 2023).

However, there is a lack of studies that aim to utilize construction and demolition waste (CDW) in the creation of artificial stones for use as finishes: kitchen and bathroom countertops, stair coverings, and more, replacing natural (ornamental) stones and even various commercially available artificial stones. Given this scenario, this research targets this niche; it seeks to substitute the standard raw material (ornamental stone waste) with CDW in the production of artificial stones. The goal is to achieve a final product that can be used similarly to ornamental stones in finishing applications, with optimized properties. The choice of a thermoset orthophthalic polyester resin for the polymer matrix was due to its cost–benefit ratio, as it initially offers satisfactory mechanical properties at the lowest market price compared to other resins. This also brings a similarity to the research, since many industrially produced composites use polyester resins, including orthophthalic ones. Resins produced with orthophthalic anhydride, known as orthophthalic resins, are commonly used due to their low cost, although they have limited thermal stability and chemical resistance [19].

A pioneering study on artificial stones was conducted in Taiwan [20], presenting the results of the production of artificial stone slabs using glass waste, stone fragments, and vacuum vibratory compaction. This research produced artificial stone slabs with unsaturated polymer resin, glass powder, and fine granite aggregates. The tests showed that the composition with 50% glass powder and 50% granite aggregates yielded the best results: compression (148.8 MPa), water absorption (below 0.02%), density (2.45), and flexural strength (51.1 MPa). In Turkey, a 2018 study produced and characterized a hybrid polymer matrix composite [21]. This research created the composite using epoxy resin, fiberglass, and granite waste, processed with a vacuum helical mixer and cast in a silicone mold. The composition named F5505, with 40% resin, 55% granite, and 5% fiberglass, achieved the best results in terms of high theoretical density, hardness, flexural strength, flexural modulus, and impact resistance. In Malaysia in 2020, another study characterized and evaluated dolomite and kaolin as fillers in the properties of poly-marble art, including twelve types of compositions with different percentages of polyester resin, dolomite, and kaolin. The best results pointed to three types of compositions: D60K15 (25% resin + 60% dolomite + 15% kaolin) with the best water absorption (0.11%); D60K10 (30% resin +

60% dolomite + 10% kaolin) with the best compression (105.43 MPa) and flexural strength (34.1 MPa); and D70% (resin + 70% dolomite) with the best Barcol hardness [22].

Among the negative impacts of the large amount of CDW generated is the rapid occupation of landfills to accommodate waste, with illegal dumping frequently used worldwide in countries such as China, Malaysia, Hong Kong, Israel, and Brazil. Major cities like Shenzhen (China) and Chennai (India), and countries like Sri Lanka have been seriously affected by disastrous events due to the improper disposal of construction waste [23].

In Brazil, the numbers related to CDW are alarming. According to the Panorama of Solid Waste in Brazil, published by the Brazilian Association of Public Cleaning and Special Waste Companies, approximately 48 million tons of construction and demolition waste (CDW) were produced in 2021 [24], This means that 38.4 million tons could be recycled or reused. The same study shows that between 10% and 30% of the construction materials purchased for a project are discarded, indicating that a significant portion of the investment in construction is wasted.

According to the Brazilian Association for the Recycling of Construction and Demolition Waste, it is estimated that in 2021, 520 kg of waste was produced per inhabitant per day. However, of the approximately 290.5 tons of debris generated daily in the country, only 21% is recycled [25].

The recycling of construction solid waste varies depending on the type of waste being treated. This research focuses on the Recycling of Construction Solid Waste and Construction and Demolition Waste, established by CONAMA Resolution 307, which pertains to Class A (inert) waste: reusable or recyclable waste such as aggregates from construction, demolitions, repairs, renovations of buildings, ceramic components, bricks, blocks, tiles, mortar and concrete, paving, and precast elements [26].

The recycling of construction waste presents advantages in the environmental, technological, and economic spheres. These advantages include the reuse of materials, reducing the use of non-renewable resources; the reduction of improper disposal; the processing of products; and cost savings by offsetting the purchase of natural raw materials.

Given the high use of concrete worldwide, the demand for aggregates of different diameters extracted from natural stones and/or riverbeds (sand and gravel) causes a range of environmental damages. Furthermore, in the not-too-distant future, the scarcity of these natural resources will become evident, which will certainly cause serious economic damage, especially to developing countries like Brazil. This problem increasingly demands research that points to new efficient and innovative uses for the various waste generated by the construction industry; this research moves in this direction.

Beyond cost efficiency, recycling contributes to the environmental goals of the industry. According to the 2022 Global Status Report for Buildings and Construction by the United Nations Environment Programme [27], carbon dioxide (CO^2) emissions from the sector reached a record 10 billion tons in 2021, 5% higher than the previous year. The 2019 Global Status Report from the International Energy Agency [28] indicates that in 2018, the construction sector was responsible for 36% of final energy use and 39% of energy- and process-related carbon dioxide emissions.

Moreover, according to the UN [29], construction is responsible for about 11% of global CO^2 emissions from human activities. This includes emissions associated with the production of building materials, the construction and demolition of buildings, and the operation and maintenance of buildings throughout their life cycle.

In this concerning context, aiming to ease the environmental pressure caused by the construction industry and the ornamental stone mining industry, this research explores new variables for the disposal of construction waste by incorporating it into the composition of artificial stones. This approach directly supports the concept of sustainable development (both environmental and economic), replacing the end-of-life concept of the linear economy with new circular flows of reuse, restoration, and renewal in an integrated circular economy process. This initiative seeks not only to reduce costs in the production of artificial stones but also to promote the large-scale, high-value use of solid waste from one of the fastest-

growing sectors on the planet, the construction industry, which predominantly disposes of its waste in landfills or dumps.

2. Materials and Methods

2.1. Materials

The construction and demolition waste (CDW) used in this research was collected from the Inert Waste Processing and Crushing Unit located at CODIN, owned by the Municipal Government of Campos dos Goytacazes (Rio de Janeiro, Brazil) under concession to Vital Engenharia S/A. The polyester resin Arazyn 25108T-10 (orthophthalic, transparent, pre-accelerated, low viscosity) from the brand Redelease (Batch: 117346) and the catalyst Mekp Butanox-M50 (methyl ethyl ketone peroxide, medium reactivity, desensitized with dimethyl phthalate), also from the brand Redelease (Batch: 151011), were both purchased locally.

2.1.1. Raw Materials Characterization

The chemical characterization of the CDW was conducted by XRF (X-ray fluorescence) at the SENAI Institute of Ceramic Technology in Criciúma, SC, Brazil, using an X-ray fluorescence spectrometer—Model: ZSX PRIMUS II (RIGAKU), following the B100-PR CR 098 method. This semi-quantitative chemical analysis provides the percentages of elements present in the material's structure.

The functional groups of the components in the polyester resin were confirmed by FTIR (Fourier-transform infrared spectroscopy) at UENF/CCT/LAMAV. The test, using a KBr pellet and resin (powder), was conducted with an IR Prestige-21 SHIMADZU equipment.

2.1.2. Development Parameters

The particle size reduction of the waste was achieved through fine sieving according to ABNT NBR 7181 [30], as shown in Table 1, to obtain three particle size ranges: coarse, medium, and fine.

Table 1. Granulometric compositions.

Class	Sieve (Mesh)	Granulometric Range (mm)
Coarse	10–40	2.000–0.420
Medium	40–200	0.420–0.075
Fine	>200	<0.075

The goal of the packing process is to find a granulometric profile of the sample to optimize the best arrangement of its particles and to determine the ideal main granulometric ranges of the waste for experimental work in the production of the proposed artificial stone.

Using the three granulometric ranges (coarse, medium, and fine), 10 particle mixtures with different compositions were proposed using the complete cubic model ternary diagram, developed based on the Simplex-Lattice Design (SLD) numerical modeling system shown in Figure 2. Each point represents a mixture of a given composition. The objective of these 10 mixtures was to find the one with the highest dry density and best packing. The ternary diagram illustrates the experimental numerical modeling simplex grid for the 10 different mixtures. Each vertex of the triangle corresponds to 100%: coarse (G), medium (M), and fine (F) particles. The other points of the triangle show (in parentheses) the corresponding fractions of the mixtures. The density of each mixture was calculated according to the Brazilian standard [31].

Statistical treatments were performed on the results of the vibrated density test using analysis of variance (ANOVA) of the completely randomized design (CRD) ($p < 0.05$) to confirm the statistical significance of the obtained data. After validating the statistical difference, the Tukey test ($p < 0.05$) was applied to corroborate the mixture that achieved the best results, chosen to produce the artificial stone plates. Factorial design is applied in various works of scientific research. Javorsky and others [32] used a full factorial

design in the study of polyvinyl chloride (PVC) adhesion to stainless steel for automotive applications. Romli and others [33] used a full factorial design, with two levels for the curing time factor and three levels for the fiber volume and compressive load factors, in a study on fiber-reinforced epoxy composite.

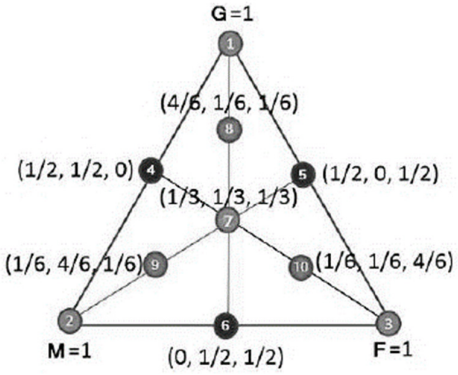

Figure 2. Ternary diagram of the simplex centroid model.

Each mixture was placed in a 1013.24 cm^3 steel container attached to a 10 kg weight, under 60 Hz vibration for 10 min. Table 2 displays the vibrated density of the 10 proposed mixtures in Figure 2.

Table 2. Vibrated density of the 10 mixtures.

Mixture	Coarse (%)	Medium (%)	Fine (%)	Vibrada Density (g/cm^3)
1	1	0	0	1.5692 ± 0.0081
2	0	1	0	1.6301 ± 0.0199
3	0	0	1	1.4936 ± 0.0047
4	1/2	1/2	0	1.7798 ± 0.0047
5	1/2	0	1/2	1.7403 ± 0.0163
6	0	1/2	1/2	1.5544 ± 0.0040
7	1/3	1/3	1/3	1.6564 ± 0.0101
8	2/3	1/6	1/6	1.7386 ± 0.0222
9	1/6	2/3	1/6	1.6482 ± 0.0201
10	1/6	1/6	2/3	1.6005 ± 0.0101

Table 3 presents the results obtained by pycnometry for the 3 mixtures with the highest dry apparent densities and consequently better packing: #4 (1/2 coarse particles and 1/2 medium particles), #5 (1/2 coarse particles and 1/2 fine particles), and #8 (4/6 coarse particles, 1/6 medium particles, and 1/6 fine particles).

Table 3. Dry apparent density—3 best mixtures.

Packaging	Coarse	Medium	Fine	Density
4	1/2	1/2	---	2.510 g/cm^3
5	1/2	---	1/2	2.308 g/cm^3
8	4/6	1/6	1/6	2.308 c/cm^3

2.2. Methods

To manufacture the artificial stones, the void volume (VV) was initially calculated using Equation (1), presented below:

Equation (1)—Void Volume (VV%)

$$VV\% = 1 - \left(\frac{\text{Dry apparent density of particles}}{\text{Residue Density}} \right) \times 100 \quad (1)$$

where the dry bulk density of the particles refers to the average packing density, and the density of the waste is the average packing density.

The minimum resin content (MRC) required to fill the void volume for the production of artificial stones is given by Equation (2), presented below:

Equation (2)—Minimum amount of resin (MAR%)

$$MAR\% = \frac{\text{VV\% } \rho \text{ resin}}{(\text{VV\% } \times \ \rho \text{ resin}) + (100 - \text{VV\%}) \times \rho \text{ waste}} \times 100 \quad (2)$$

where ρ resin is the density of the resin and ρ residue is the density of the residue.

After determining VV and MRC, a resin content of 15% was found necessary for manufacturing artificial stone slabs from both batches (4, 5, and 8), as shown in Table 4. This percentage directly considers the wettability in the residue/resin interaction process. In practice, some resin is lost during transfer from the measuring container to the mixing system, and the choice of polyester resin itself, where the catalyst is used in a ratio of only 1%, limits the liquid part of the mixture.

Table 4. Values (VV% and MAR%).

Packaging	VV%	MAR%
4	29.09	13.14
5	24.67	12.22
8	24.67	12.22

2.2.1. Development Parameters of Artificial Rocks Slabs

The CDW, as specified in Table 1 for particle size distribution, was dried in a 100 °C oven for 24 h to remove moisture, weighed in the appropriate proportions as per Table 2, and then fed into an automatic cylindrical mixer with polyester resin and catalyst at ratios of 85% CDW and 15% resin by mass, respectively. The mixture was poured into a metal mold to create slabs measuring 100 mm × 100 mm × 10 mm, connected to a vacuum system (600 mmHg), and placed on a vibrating table for 2 min. This step facilitates air removal from the grain interstices, enhancing resin wetting and particle distribution [34]. The mold, still under vacuum, was then transferred to a hydraulic press and compressed at 10 MPa for 20 min at 90 °C to aid resin curing [35].

After compaction, the slabs were demolded, excess material was trimmed, and they were placed in a 100 °C oven for 24 h for post-curing. Subsequently, the slabs were cut to the dimensions required for the proposed tests using a diamond blade, as shown in Figure 3.



Figure 3. Stages of manufacturing artificial stone slabs: (1) mixer; (2) vacuum molding in the mixer; (3) vacuum molding on the shaker; (4) vacuum compaction molding.

2.2.2. Physical Properties of the Plates (Packaging 4, 5 and 8)

Through ANOVA statistical treatment and Tukey's test, which involves comparing all possible pairs of means and is based on the least significant difference, considering the percentile of the group, where variance and multiple comparison among means of experiments were analyzed, packaging (compositions) 4, 5, and 8 yielded the best results (more compacted mixtures). For the physical index tests, 10 specimens of 50 mm × 50 mm × 10 mm were cut from artificial stone slabs of each packaging 4, 5, and 8. Apparent density, water absorption, and apparent porosity were determined according to ABNT/NBR 15845-2 [36], as expressed in Figure 4.

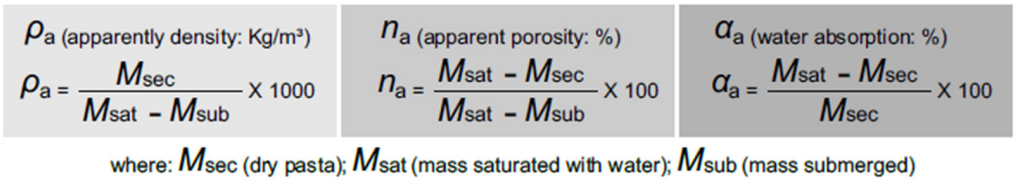

Figure 4. Expressions for determination: apparent density, water absorption and apparent porosity.

2.2.3. Mechanical Property (Bending Due to Three-Point Loading) of the Plates (Packaging 4, 5 and 8)

Seven specimens from each mix (4, 5, and 8), with dimensions of 100 mm × 25 mm × 10 mm, were subjected to three-point bending tests according to ABNT/NBR 15845-6 [37]. The tests were conducted using an INSTRON 5582 universal testing machine at UENF/CCT/LAMAV, with a crosshead speed of 0.25 mm/min, a load cell capacity of 100 KN, and a support span of 80 mm. The three-point bending test is crucial for evaluating the mechanical properties of materials under applied loads that induce bending. It plays a key role in analyzing the structural behavior of artificial stones, assessing their strength, stiffness, and load-bearing capacity.

2.2.4. Mechanical Property (Bending by Three-Point Loading) of Polyester Resin

For comparative purposes, a three-point flexural test was performed on the polyester resin used in this research. Eight specimens measuring 60 mm × 12 mm × 10 mm were prepared and tested according to ASTM D790 (ASTM D790-15, 2016) on an INSTRON 5582 universal testing machine at UENF/CCT/LAMAV, with a crosshead speed of 2 mm/min, a load cell capacity of 100 KN, and a support span of 60 mm.

Composition 5 (1/2 coarse particles and 1/2 fine particles) demonstrated superior compaction and mechanical strength in preliminary tests, leading this composition, now renamed as CDW-5, to be selected for further detailed studies in the research.

2.2.5. Characterization of Artificial Rock RCD-5

The fracture surface of CDW-5, subjected to the bending test, was examined using SEM (Scanning Electron Microscope) for microstructural analysis. The test was conducted at UENF/CCT/LAMAV on a Super Scan SSX-550 from SHIMADZU, with 15 kV of secondary electrons. A microstructural analysis is crucial for assessing the bonding quality between CDW particles and polyester resin, as well as identifying void presence. For comparative purposes, the fractures of compositions 4 and 8 were also microstructurally analyzed. The CDW powder, with granulometry detailed in Table 1, was also SEM-examined for morphological analysis.

Uniaxial compression strength testing was performed on 8 specimens sized 25 mm × 25 mm × 25 mm, following ABNT/NBR 15845-5 [38] in UENF/CCT/LAMAV using an INSTRON 5582 universal testing machine, with a crosshead speed of 0.25 mm/min and a 100 KN load cell.

Chemical resistance testing was conducted according to ABNT/NBR 16596 [39]. The test involved 10 specimens sized 50 mm × 50 mm × 10 mm. Specimens were exposed

to 5 reagents for 24 h and 4 reagents for 96 h, with one specimen in contact with distilled water for 96 h in the artificial stone laboratory at UENF/CCT/LAMAV.

Thermal analysis was determined by dilatometry at UENF/CCT/LAMAV. Dimensional variations of a specimen sized 7 mm × 7 mm × 10 mm under heating conditions were evaluated as per ABNT NBR 15845-3 [40]. The test was conducted using the Netzsch DIL402PC equipment, with a heating rate of 10 °C/min and a temperature range of 30–350 °C.

As a final presentation, three slabs were prepared with sanding, waterproofing, and polishing as final finishes to best depict the envisioned artificial stone in the study, comprising CDW and resin, as a high-quality product for kitchen countertops or flooring. The slabs were produced in natural form, with black and white pigmentation.

3. Results and Discussion

3.1. XRF Chemical Characterization of CDW

Table 5 presents, in percentages, the chemical composition of the construction and demolition waste (CDW) determined by XRF. The composition is primarily composed of oxides: Al_2O_3, CaO, and SiO_2, accounting for 77.63% of the total. This composition was expected, due to the waste's high content of concrete and asphalt waste, essential for its intended use as a base and sub-base material in municipal road construction, a key factor that enhances the viability of using this waste in artificial stone production, as most CDW recycling plants have a significant demand for such applications (aggregates for bases).

Table 5. Chemical analysis by XRF (civil construction and demolition waste).

Determination of Chemical Analysis by XRF Spectrometry–PR-CR-098 (Sample: CDW) %									
Al_2O_3	CaO	Fe_2O_3	K_2O	MgO	Mno	Na_2O	P_2O_5	SiO_2	
9.752	22.308	3.276	1.782	1.948	0.056	1.007	0.219	45.568	
TiO_2	BaO	Co_2O_3	PbO	SrO	ZnO	ZrO_2/Hf	CI	SO_3	Fire Loss
0.472	0.061	<0.050	<0.050	0.111	<0.050	<0.050	0.891	2.533	9.987

The chemical composition of CDW shares similarities with clinker (Table 6), which forms the basis of cement composition [41].

Table 6. Chemical composition of clinker.

Chemical Composition—Clinker (%)						
CaO	SiO_2	Al_2O_3	Fe_2O_3	MgO	Na_2O	SO_3
61–67	17–24	3–8	1–6	0.1–4	0.5–1.5	1–3

Another portion of CDW's composition, comprising 10.54%, includes Fe_2O_3, SO_3, Na_2O, K_2O and MgO.

3.2. Characterization of Resin's Functional Groups (Fourier Transform Infrared Spectroscopy)

The Fourier transform infrared spectrum, shown in Figure 5, depicts the characteristic bands of the functional groups present in the polymer, detailed in Table 7.

The band at 744 cm^{-1} in the FTIR spectrum is attributed to ortho-substituted benzene, indicating the presence of phthalic anhydride in the resin to control crosslinking. The double bond facilitates crosslinking, enhancing the material's mechanical strength.

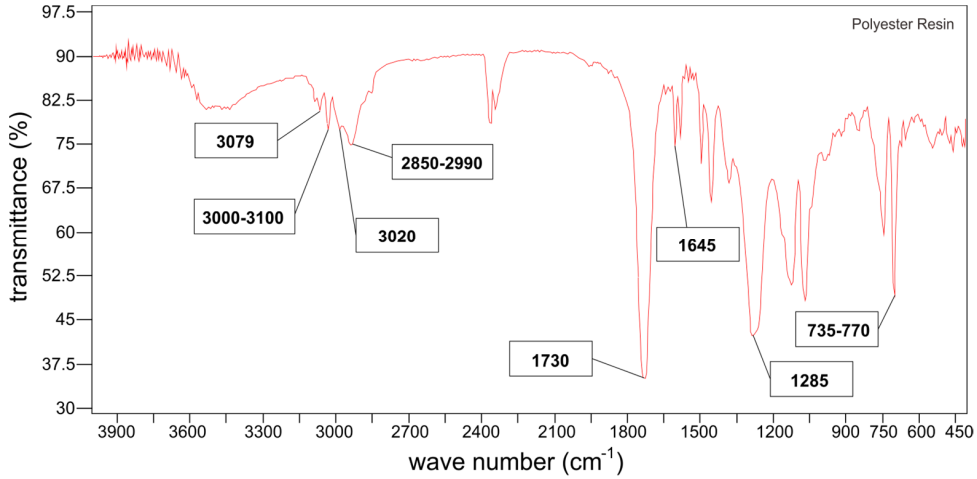

Figure 5. Fourier transform infrared spectrum (polyester resin).

Table 7. Characteristic bands of functional groups—polyester resin.

Wave Number	Bands
3000–3100	Aromatic C-H stretch
3079	Stretch = asymmetrical CH_2
3020	Stretch = asymmetrical CHR
2990–2850	$-CH_3$ e $-CH_2$
1730	Stretch = CH_2
1645	RCH = CH_2
1285	C-0 ester stretch
770–735	Replaced ortho benzene

3.3. Physical Physical Indices and 3-Point Bend Strength

Table 8 shows the physical indices and the results of 3-point bend test among the top 3 mixtures (4, 5, and 8), confirming the composition 5 (1/2 coarse particles and 1/2 fine particles) as the one with better compaction and mechanical strength (Figure 6).

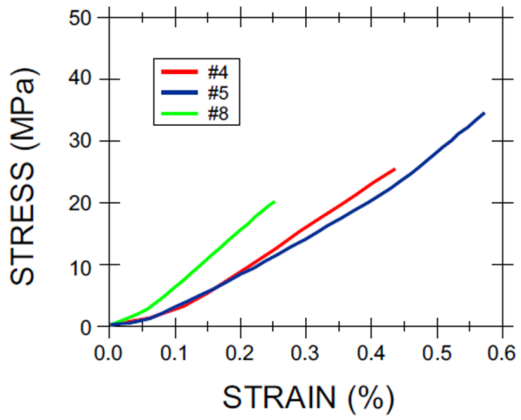

Figure 6. Diagram (bending rupture stress x bending deformation) of compositions 4, 5 and 8.

Table 8. Physical indices and 3-point flexion.

Composition	Density Apparent Ꝑa (g/cm^3)	Porosity Apparent ηa (%)	Water Absorption αa (%)	Volume M^3	Plates Inflection MPa
#4	2.129	1.46	0.66	0.0309	24.66
1/2 coarse +1/2 medium	±0.12	±0.30	±0.14	±0.002	±2.31
#5	2.256	1.55	0.69	0.0296	34.74
1/2 coarse +1/2 fine	±0.10	±0.28	±0.13	±0.002	±2.55
#8	2.252	2.32	1.03	0.0308	20.55
2/3 coarse +1/6 medium +1/6 fine	±0.98	±0.28	±0.13	±0.001	±2.41

3.4. Flexural Strength from 3-Point Bending (CDW-5 and Resin)

Table 9 presents the maximum flexural strengths due to the 3-point loading of CDW-5 artificial stone and polyester resin.

Table 9. Three-point flexural strength: RCD-5 and polyester resin.

Material	3-Point Flexural Strength
CDW-5	34.74 MPa ± 2.55
Polyester Resin	80.24 MPa ± 7.74

Figure 7 illustrates the stress–strain curves obtained from the 3-point bending test of the artificial stone CDW-5 and polyester resin. Mechanical strength, or the stress at which the material fractures, is the most critical property of structural materials [42].

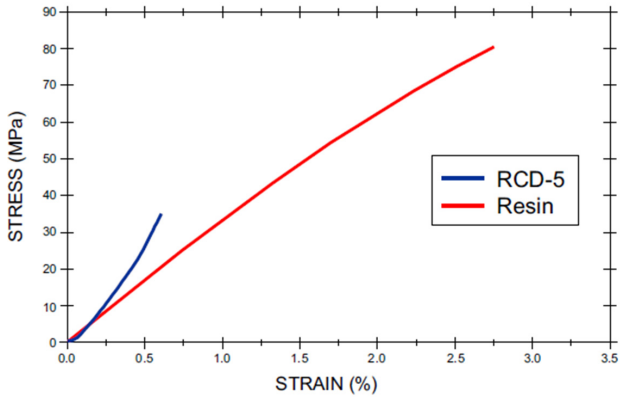

Figure 7. Diagram (bending rupture stress x bending deformation) of RCD-5 and polyester resin.

The hydration reaction of CDW in the presence of resin aims to form hydrated calcium silicates and calcium hydroxide. In the presence of calcium sulfate, a substance called ettringite is formed, which is a hydrated mixed oxide of calcium, aluminum, and iron commonly associated with sulfate ions, as identified in the CDW characterization by XRF. This substance is crucial, as it forms chemical bonds with other substances, contributing to its hardening [43].

Comparing the result (34.74 MPa ± 2.55) obtained from the 3-point bending flexural strength test of artificial stone CDW-5 with other similar artificial stones found in the literature, including Lee et al. [20], 27.9–52.7 MPa; Ribeiro et al. [44], 21.5 MPa; Hamizah et al. [22], 34.1 MPa; and Peixoto et al. [45], 25.4 MPa; the consistent performance standard of CDW-5 can be observed.

The ABNT/NBR 15845-6 [37] standard specifies a minimum flexural strength of 10 MPa for stones used in flooring, while ASTM C503 [46] sets a value of 7 MPa. According to Chiodi Filho and Rodriguez [47], ornamental stones used in construction with flexural

strengths above 20 MPa are classified as high-strength materials. CDW-5 demonstrated a flexural strength exceeding this threshold (347.40 kg/cm^2), qualifying it as a high-strength artificial stone suitable for applications such as kitchen countertops and service areas.

3.5. Uniaxial Compression Strength

Figure 8 shows the maximum uniaxial compressive strength of CDW-5.

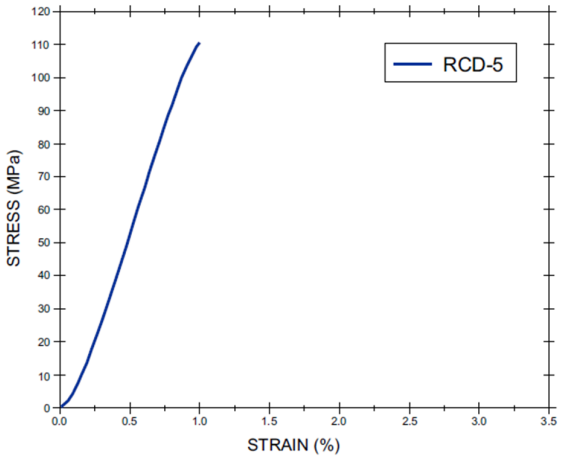

Figure 8. Diagram (stress x strain—compression) of CDW-5.

When comparing the result (111.96 MPa + 5.24) obtained from the uniaxial compressive strength of artificial stone CDW-5 with similar results found in the literature, including Lee et al. [20], 78.70–151.30 MPa; Ribeiro et al. [44], 77.9 MPa; Hamizah et al. [22], 105.43 MPa; and Agrizzi et al. [48], 100.70 MPa, we observe consistent performance in both flexural and compressive strength, affirming the robust performance of CDW-5 in preliminary research.

Once again, according to Filho and Rodriguez [47], ornamental stones used as cladding in construction, with a uniaxial compressive strength ranging between 700 and 1300 kg/cm^2, are classified as medium-strength materials. CDW-5 demonstrated a uniaxial compressive strength of 1119.60 kg/cm^2, underscoring its potential for use in construction applications.

3.6. Scanning Electron Microscopy (SEM) Analysis

Figures 9–11 present the micrographs of the particle sizes of CDW (fine, medium, and coarse) used in this research, obtained by SEM.

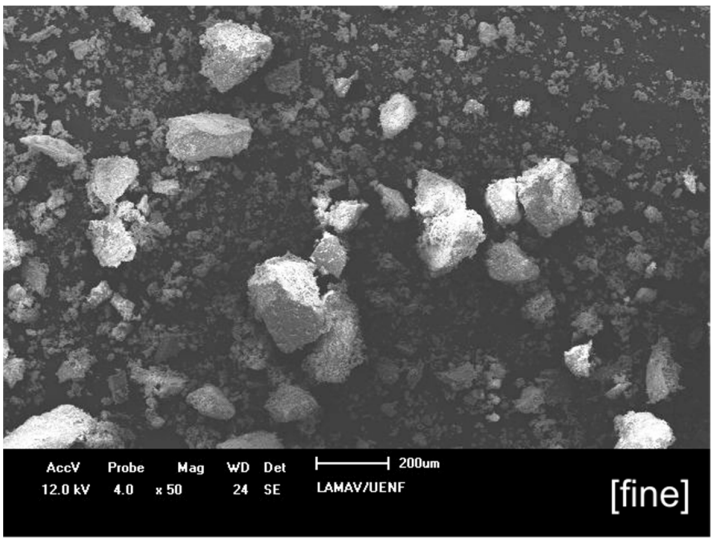

Figure 9. Micrograph CDW—particle size: fine (×50).

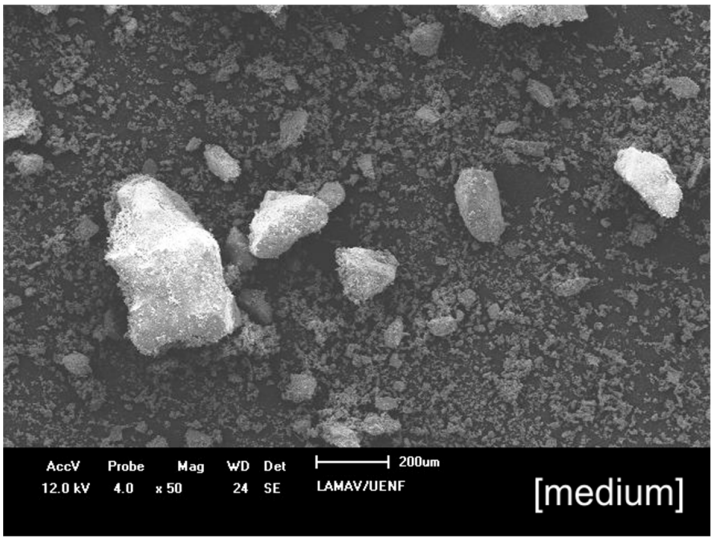

Figure 10. Micrograph CDW—particle size: medium (×50).

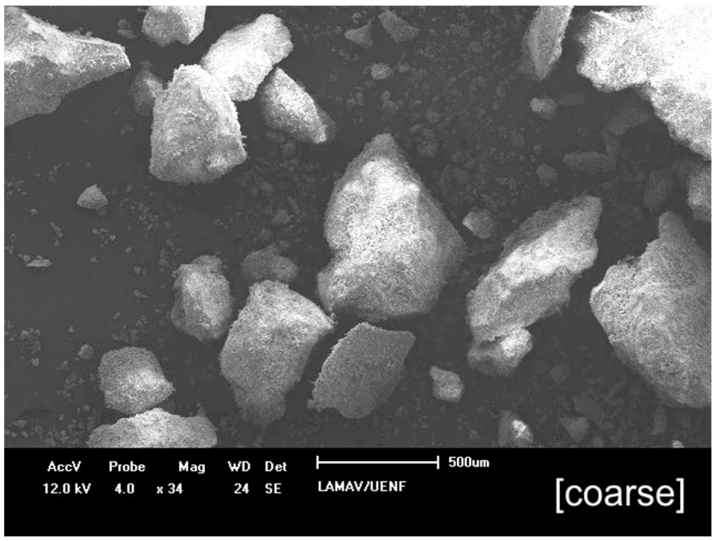

Figure 11. Micrograph of CDW—coarse granulometry (×34).

In both micrographs, the morphology of the grains can be observed, showing rough surfaces, irregular shapes, and protrusions along the contours. The shape of the grains, surface roughness, and protrusions contribute to higher mechanical strength values, as these characteristics not only enhance internal locking but also improve adhesion between the resin and the grains.

Figure 12 shows how the morphology of the coarse CDW grains interlock like a puzzle, forming a natural compaction as the voids are subsequently filled by the fine granulometry.

The morphology of the particles can alter the packing condition. The less spherical a particle is, the lower the packing density of a distribution containing it, as friction occurs between particles due to contact between their irregular surfaces. The smaller the size of the irregular particles, the greater this effect, due to the higher specific surface area [49].

Figure 13 presents the micrographs, obtained by SEM, of the fracture surfaces of the specimens (compositions 4, 5 and 8) from the bend test.

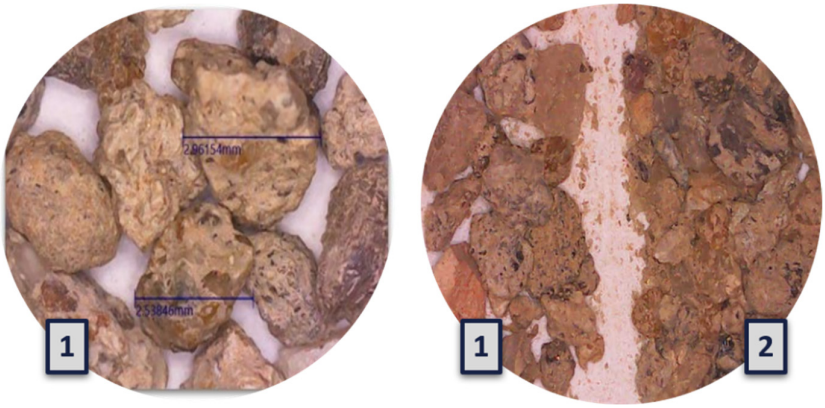

Figure 12. CDW Digital Micrograph: (1) coarse grain size; (2) packaging—coarse/fine granulometry.

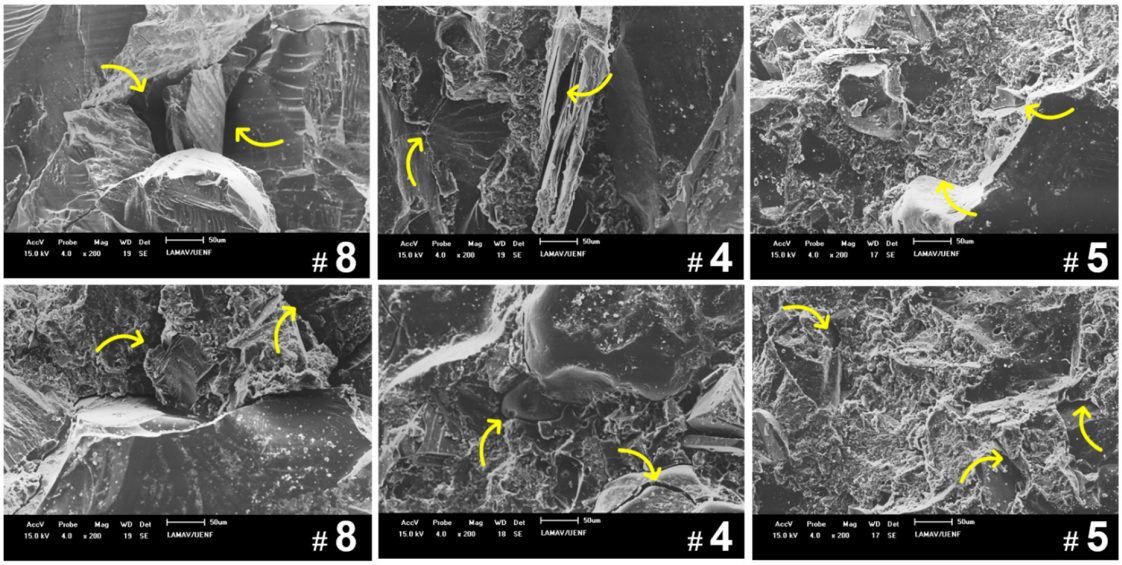

Figure 13. Micrographs of fractures: compositions—8, 4 and 5 (×200); where the yellow arrows point to the cracks and their proportions.

The progression of packing is evident in the sequence of micrographs. Composition 8 shows cracks along the anchorage between the reticulations, and the interaction with the resin leaves void spaces along the fracture. Composition 4 shows improved behavior compared to composition 8; its cracks are smaller, and the waste/resin interaction has better adhesion, resulting in a more positive outcome compared to composition 8. However, composition 5, even with some micro-failures on the analyzed surface, shows the significantly better anchorage of the reticulated structure to the polymer matrix. The resin coating is more efficient with the proposed granulometry for this composition, leading to better density and mechanical strength results. The quality of the interfacial interaction is directly related to the improvement of the mechanical strength of a composite. This is because good interfacial wettability means higher adhesive strength [50].

3.7. Chemical Attack Resistance

The reagents used in this test simulate the chemical composition of various substances found in food and general cleaning products.

Observing the results presented in Figure 14, we can note chromatic modifications in several test specimens that were exposed for 24 h, as well as for 96 h. Exceptions are the test specimens 01 (ammonium chloride), 02 (sodium hypochlorite), and 10 (distilled water).

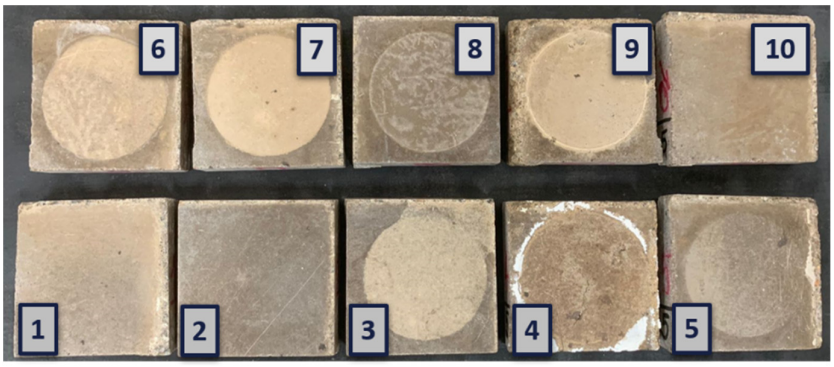

Figure 14. Chromatic modifications—test specimens: (1) ammonium chloride; (2) sodium hypochlorite; (3) citric acid; (4) lactic acid; (5) acetic acid; (6) 3% hydrochloric acid; (7) 18% hydrochloric acid; (8) potassium hypochlorite 30 g/L; (9) potassium hypochlorite 100 g/L; (10) distilled water.

These chromatic modifications can be explained by the composition of the orthophthalic polyester resin. Orthophthalic acid or its anhydride is used as a modifier, making its chemical properties inferior to others due to the difficulty in obtaining high molecular weight polymers (short molecular chains—Figure 15). Phthalic anhydride has a strong tendency to regenerate from the half-esters of phthalic acid (reversible reaction), which increases the presence of low molecular weight species that are highly sensitive to chemical attack [51].

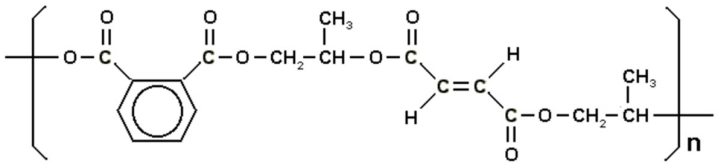

Figure 15. Orthophthalic polyester molecular chain.

Table 10 presents the results of the visual inspection of the effects of a chemical attack by a reagent, as outlined by the NBR standard that guides the test. It is noted that there is an absence of dissolution and mineral detachment.

Table 10. Effects of a chemical attack by a reagent.

CP	Reagent	Exposure	Modification Chromatic	Dissolution	Detachment Mineral
1	Ammonium Chloride	24 h	absent	absent	absent
2	Sodium Hypochlorite		absent	absent	absent
3	Citric Acid		present	absent	absent
4	Lattic Acid		present	absent	absent
5	Acetic Acid		present	absent	absent
6	Hydrochloric Acid 3%	96 h	present	absent	absent
7	Hydrochloric Acid 18%		present	absent	absent
8	Potassium Hypochlorite 30 g/L		present	absent	absent
9	Potassium Hypochlorite 100 g/L		present	absent	absent
10	distilled water		absent	absent	absent

A specific observation is necessary regarding the effect of chemical attack on specimen N° 4, which was exposed to lactic acid for 24 h. In addition to the chromatic modification,

an irregular white layer formed from the liquid part, which may have leaked from the container onto the specimen during the test period. This irregular form likely resulted from the oxidation reaction of the primary carbon present in the reagent [52]. There was no mineral detachment, as observed in Figure 16.

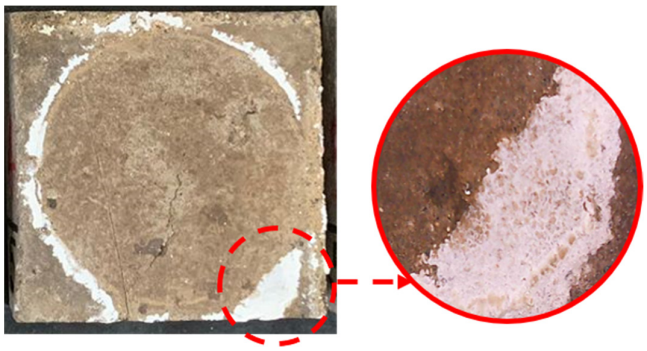

Figure 16. Digital microscopy (Detail chemical attack N. 04—lactic acid).

3.8. Thermal Analysis by Dilatometry

The dilatometric analysis measures the dimensional changes (contraction and expansion) that a material undergoes, as a function of temperature, when subjected to a controlled program of temperature in controlled atmosphere. In the development of artificial stone, thermal transformations occur in the curing phase due to the matrix/residue polymerization reaction [53]. Figure 17 presents the dilatometric curve of the artificial stone CDW-5.

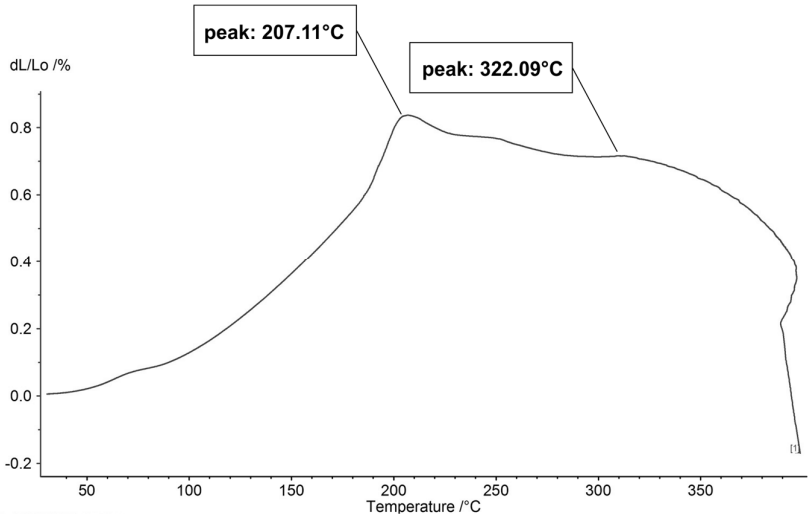

Figure 17. CDW-5 dilatometric curve.

We can observe the structural behavior in a heated environment in the temperature range of 0–350 °C. In the range of 0–200 °C, the materials are adapting to the heated environment, expanding the pores and causing the structure to lose moisture. The first peak occurs at 207 °C, where until the temperature of 322 °C (second peak), the material undergoes contraction. From the second peak onward, the material starts to decompose slowly, with weight loss, mostly from the resin, as reported in other research [54]. Chiodi Filho and Rodriguez [47] indicate that ornamental stones used as coverings in civil construction, with a thermal expansion coefficient between 8–10, are considered of medium standard, where CDW-5 presented a coefficient of 8.33.

3.9. Final Product (Prototype)

Figure 18 shows the slabs that received final finishing (sanding, waterproofing, and polishing) to better represent the proposed artificial stone produced with CDW and polyester resin for use in kitchen countertops, leisure areas, and bathrooms, as well as for cladding on stairs, for example.

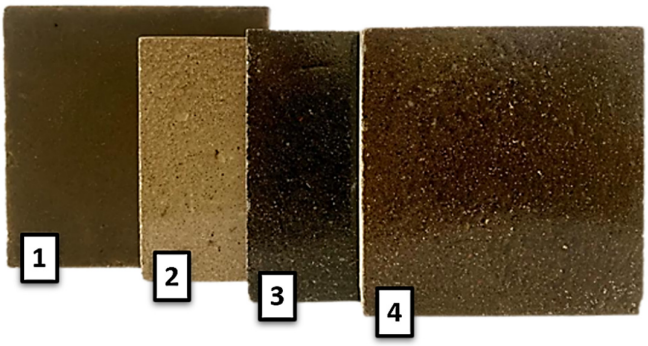

Figure 18. CDW-5 artificial stone: (1) raw slab; (2) white pigment stone; (3) black pigment stone; (4) natural stone.

3.10. Applicability

As a final note, through the website of the Brazilian Association of the Ornamental Rocks Industry (ABIROCHAS, 2024), we can determine the applications of CDW-5 based on the section "Specification and Application Guides for Ornamental and Cladding Stones", and the results of physical and mechanical indices tests (3-point bending and compression), as shown in Tables 11 and 12.

Table 11. Adapted application (CDW-5).

Rocks for Coating of Tops/Countertops *		
Type of Coating	Technological Parameters	
Tops/Countertops	Water Absorption (>0.4%)	Rupture Module (>8 MPa)
Class	Possibilities of Using the Rock Evaluated	
A2D1	• The application of sealant hydro–oil repellent on the face and edges of kitchen and bathroom sinks is necessary, as well as on counters and bar tables, bakeries and congeners.	

(*) Plates with minimum thickness of 2 cm.

Table 12. Adapted application (CDW-5).

Flooring Rocks		
Type of Coating	Technological Parameters	
Floors	Water Absorption (>0.4%)	Amsler Abrasive Wear (0.85 mm to 2 mm)
Class	Possibilities of Using the Rock Evaluated	
A2B2	• Residential and commercial areas, only with eventual wetting. • Residential areas have low pedestrian traffic. Commercial areas have medium pedestrian traffic. Public areas have high pedestrian traffic. • Internal social environments (rooms and bedrooms) and commercial (offices, shops, offices, etc.) receive occasional wetting. Indoor service environments, kitchens and baths, and outdoor environments, receive frequent wetting.	

3.11. Comparative

Table 13 presents comparative data between the results of the apparent density, water absorption, flexural strength, and compression strength of CDW-5 and the artificial stones produced in various studies.

Table 13. CDW-5 X artificial rocks found in the literature.

Authors	Apparent Density (g/cm³)	Water Absorption (%)	Flexural Strength (MPa)	Compressive Strength (MPa)
Lee, M. Y. et al., [20]	2.05–2.44	0.01–0.2	27.9–52.7	78.70–151.30
Ribeiro, C. E. G. et al., [34]	2.27 ± 0.02	0.19 ± 0.02	4.21 ± 0.52	14.17 ± 1.03
Carvalho et al., [35]	2.68 ± 0.03	0.17 ± 0.04	57.57 ± 3.21	N.D.
RMC Tradicional [55]	2.52–2.57	0.09–0.32	13.6–17.2	97–131
Carvalho et al., [56]	2.35 ± 0.08	0.35 ± 0.09	30 ± 1.44	N.D.
Peng, L. et al., [57]	2.41	0.01	73.5	170.9
Gomes et al., [58]	2.12 ± 0.01	0.38 ± 0.06	30 ± 3	N.D.
Hamizah et al., [22]	N.D.	0.11	34.10	105.43
Carvalho et al., [53]	2.24	0.19	32.0	N.D.
Silva et al., [59]	N.D.	0.13	32.77	N.D.
Barreto et al., [16]	2.22	0.11	34.36	N.D.
CDW-5	2.25	0.69	34.74	111.96

(N.D.) undisclosed value.

4. Conclusions

Through this research, an artificial stone finish named CDW-5 was developed using construction and demolition waste and orthophthalic polyester resin in proportions of 85% and 15%, respectively, processed via vibration, compression, and vacuum systems. Based on the results presented, the following conclusions can be drawn:

- Construction and demolition waste, being heterogeneous due to the diversity of materials collected, must primarily consist of concrete and asphalt residues to meet chemical composition parameters, ensuring expected outcomes.
- CDW-5's composition proves to be lightweight with a density of 2.256 g/cm^3, reducing transportation costs and industrial production expenses. Its porosity (1.55%) and water absorption (0.69) classify CDW-5 as a medium-quality cladding material suitable for wet environments, necessitating effective waterproofing and polishing processes for such applications.
- Mechanical tests yielded results surpassing those of many other studies in the field. A flexural strength of 34.74 MPa ± 2.55 categorizes CDW-5 as a high-quality material, exceeding the >20 MPa threshold, while a compressive strength of 111.96 MPa ± 5.24 places it in the medium-quality range. Scanning electron microscopy (SEM) images of composition 5 confirm excellent matrix/particle adhesion.
- Chemical resistance testing highlights CDW-5's vulnerability without proper waterproofing and polishing treatments for everyday use. The use of orthophthalic polyester resin in this research, due to its lower chemical resistance properties compared to other resins, was chosen for its cost-effectiveness despite its vulnerability to chemical attack. Future research should explore resins with enhanced chemical resistance and thermal properties.
- Overall, CDW has significant potential as a raw material for artificial stone production, aligning with sustainable development principles (both environmental and economic). It reintroduces a waste product, widely disposed of in landfills worldwide, into the production cycle, shifting from a linear economy end-of-life concept to circular reuse,

restoration, and renewal processes integrated into the circular economy. Additionally, CDW-5 exhibits properties comparable to commercially available artificial stones, enhancing the quality of the final product.

Author Contributions: Conceptualization, M.B.R., H.A.C.L., C.M.F.V., E.A.S.C. and S.N.M.; Methodology, M.B.R. and C.M.F.V.; Software, M.B.R. and E.A.S.C.; Validation, M.B.R., H.A.C.L., C.M.F.V., A.R.G.A., E.A.S.C. and S.N.M.; Formal analysis, M.B.R., H.A.C.L., C.M.F.V. and E.A.S.C.; Investigation, M.B.R.; Resources, M.B.R., H.A.C.L., C.M.F.V. and A.R.G.A.; Data curation, M.B.R.; Writing—original draft, M.B.R. and E.A.S.C.; Writing—review & editing, M.B.R., C.M.F.V., A.R.G.A. and S.N.M.; Visualization, M.B.R., A.R.G.A. and E.A.S.C.; Supervision, H.A.C.L. and C.M.F.V.; Project administration, H.A.C.L. and C.M.F.V.; Funding acquisition, S.N.M. All authors have read and agreed to the published version of the manuscript.

Funding: This research received no external funding.

Data Availability Statement: Data is contained within the article.

Conflicts of Interest: The authors declare no conflict of interest.

References

1. Varshney, H.; Khan, R.A.; Khan, I.K. Sustainable use of different wastewater in concrete construction: A review. *J. Build. Eng.* **2021**, *41*, 102411. [CrossRef]
2. Galetakis, M.; Soultana, A. A review on the utilisation of quarry and ornamental stone industry fine by-products in the construction sector. *Constr. Build. Mater.* **2016**, *102*, 769–781. [CrossRef]
3. Salman Rais, M.; Ahmad Khan, R. Effect of biomineralization technique on the strength and durability characteristics of recycled aggregate concrete. *Constr. Build. Mater.* **2021**, *290*, 123280. [CrossRef]
4. Hamada, H.M.; Thomas, B.S.; Yahaya, F.M.; Muthusamy, K.; Yang, J.; Abdalla, J.A.; Hawileh, R.A. Sustainable use of palm oil fuel ash as a supplementary cementitious material: A comprehensive review. *J. Build. Eng.* **2021**, *40*, 102286. [CrossRef]
5. Miranda de Souza, A.; Soares de Lima, G.E.; Nalon, G.H.; Salgado Lopes, M.M.; Luís de Oliveira Júnior, A.; Rodrigues Lopes, G.J.; de Andrade Olivier, M.J.; Pedroti, L.G.; Ribeiro, J.C.L.; de Carvalho, J.M.F. Application of the desirability function for the development of new composite eco-efficiency indicators for concrete. *J. Build. Eng.* **2021**, *40*, 102374. [CrossRef]
6. Ferreira, R.L.S.; Anjos, M.A.S.; Pinto, L.M.C.; de Azevedo, A.R.G.; de Brito, J. Long-term analysis of the physical properties of the mixed recycled aggregate and their effect on the properties of mortars. *Constr. Build. Mater.* **2021**, *274*, 121796. [CrossRef]
7. Mendes, B.C.; Pedroti, L.G.; Fontes, M.; Ribeiro, J.C.L.; Vieira, C.M.F.; Pacheco, A.A.; de Azevedo, A.R. Technical and environmental assessment of the incorporation of iron ore tailings in construction clay bricks. *Constr. Build. Mater.* **2019**, *227*, 116669. [CrossRef]
8. Lamônica, C.H.; Azambuja, M.D.A.; Battistelle, R.A.G. Gestão dos Resíduos Sólidos da Construção Civil: Um estudo bibliométrico na base Scopus e Web of Science (2009–2019). *Rev. Nac. Gerenciamento Cid.* **2019**, *7*, 989–1001. [CrossRef]
9. Xia, B.; Ding, T.; Xiao, J. Life cycle assessment of concrete structures with reuse and recycling strategies: A novel framework and case study. *Waste Manag.* **2020**, *105*, 268–278. [CrossRef] [PubMed]
10. Ossa, A.; García, J.L.; Botero, E. Use of recycled construction and demolition waste (CDW) aggregates: A sustainable alternative for the pavement construction industry. *J. Clean. Prod.* **2016**, *135*, 379–386. [CrossRef]
11. Rodrigues, F.; Carvalho, M.T.; Evangelista, L.; de Brito, J. Physical–chemical and mineralogical characterization of fine aggregates from construction and demolition waste recycling plants. *J. Clean. Prod.* **2013**, *52*, 438–445. [CrossRef]
12. Rodrigues, F.; Valle, S.; Gonçalves, P.C.; Ranieri, G.A.M.; Melo, M.d.L.N.M.; Santos, V.C.d. Use of recycled aggregates from civil construction in self-compacting mortar. *Rev. IBRACON De Estrut. E Mater.* **2021**, *15*, e15107.
13. Ferreira, R.L.S.; Anjos, M.A.S.; Pereira, J.E.S.; Fonseca, N.J.M.; Nóbrega, A.K.C. Avaliação das propriedades físicas, químicas e mineralógicas da fração fina (<150 µm) do agregado reciclado de RCD. *Cerâmica* **2019**, *65*, 139–146.
14. Carneiro, A.P.; Brum, I.A.S.; Cassa, J.C.d.S. *Reciclagem de Entulho Para a Produção de Materiais de Construção–Projeto Entulho Bom*; EDUFBA: Salvador, Brasil, 2001.
15. Fagury, S.C.; Fernando, M.G. Gestão de resíduos de construção e demolição (RCD)—Aspectos gerais da gestão pública. *Exacta* **2007**, *5*, 35–45.
16. Nunes Sales Barreto, G.; Pessanha Menezes Gomes, M.L.; Santos Carvalho, E.A.; Colorado Lopera, H.A.; Neves Monteiro, S.; Fontes Vieira, C.M. Flexible artificial stone developed with waste tire and waste glass agglomerated by a biopolymeric resin. *J. Mater. Res. Technol.* **2023**, *25*, 7417–7429. [CrossRef]
17. Lee, G.-W.; Lee, N.-J.; Jang, J.; Lee, K.-J.; Nam, J.-D. Effects of surface modification on the resin-transfer moulding (RTM) of glass-fibre/unsaturated-polyester composites. *Compos. Sci. Technol.* **2002**, *62*, 9–16. [CrossRef]
18. ABIROCHAS. Associação Brasileira da Indústria de Rochas Ornamentais. 2024. Available online: https://abirochas.com.br/ (accessed on 6 October 2022).

19. Cheremisinoff, N.P. Processing of Unsaturated Polyesters. In *Advanced Polymer Processing Operations*; William Andrew: Norwich, NY, USA, 1998; pp. 1–38.
20. Lee, M.-Y.; Ko, C.-H.; Chang, F.-C.; Lo, S.-L.; Lin, J.-D.; Shan, M.-Y.; Lee, J.-C. Artificial stone slab production using waste glass, stone fragments and vacuum vibratory compaction. *Cem. Concr. Compos.* **2008**, *30*, 583–587. [CrossRef]
21. Açıkbaş, G.; Özcan, S.; Açıkbaş, N. Production and characterization of a hybrid polymer matrix composite. *Polym. Compos.* **2018**, *39*, 4080–4093. [CrossRef]
22. Hamizah, A.; Rashita, A.; Malek, S. Characterization and evaluation of dolomite and kaolin as filler on the properties of poly art marble. *Mater. Today Proc.* **2020**, *29*, 173–178. [CrossRef]
23. Duan, Z.; Poon, C.S. Properties of recycled aggregate concrete made with recycled aggregates with different amounts of old adhered mortars. *Mater. Des.* **2014**, *58*, 19–29. [CrossRef]
24. ABREMA. Associação Brasileira de Resíduos e Meio Ambiente. 2024. Available online: https://www.abrema.org.br/ (accessed on 1 March 2024).
25. ABRECON. Associação Brasileira Para Reciclagem de Resíduos da Construção Civil e Demolição—Abrecon. 2023. Available online: https://abrecon.org.br/ (accessed on 7 April 2024).
26. CONAMA N.307. Estabelece Diretrizes, Critérios e Procedimentos Para a Gestão dos Resíduos da Construção Civil. 2023. Available online: http://conama.mma.gov.br/ (accessed on 13 October 2023).
27. UNEP.ORG. *2023 Global Status Report for Buildings and Construction: Beyond Foundations—Mainstreaming Sustainable Solutions to Cut Emissions from the Buildings Sector*; United Nations Environment Programme: Nairobi, Kenya. 2024. Available online: https://wedocs.unep.org/20.500.11822/45095 (accessed on 13 October 2023).
28. IEA.ORG. International Energy Agency. 2024. Available online: https://www.iea.org (accessed on 2 March 2024).
29. UN.ORG. United Nations Organization. 2024. Available online: https://www.un.org/ (accessed on 1 April 2024).
30. *ABNT NBR 7181*; Solo—Análise Granulométrica. Associação Brasileira de Normas Técnicas: Rio de Janeiro, Brazil, 2016.
31. *ABNT NBR MB 3388*; Determinação do Índice Mínimo de Índice de Vazios de Solos Não Coesivos—Método de Ensaio. Associação Brasileira de Normas Técnicas: Rio de Janeiro, Brazil, 1991.
32. Javorsky, J.; Franchetti, M.; Zhang, H. Determining the optimal parameters of bonding polyvinylchloride to stainless steel in automotive applications with the use of full factorial design of experiment. *CIRP J. Manuf. Sci. Technol.* **2014**, *7*, 151–158. [CrossRef]
33. Romli, F.I.; Alias, A.N.; Rafie, A.S.M.; Majid, D.L.A.A. Factorial Study on the Tensile Strength of a Coir Fiber-Reinforced Epoxy Composite. *AASRI Procedia* **2012**, *3*, 242–247. [CrossRef]
34. Ribeiro, C.E.G.; Rodriguez, R.J.S.; Vieira, C.M.F.; de Carvalho, E.A.; Candido, V.S.; Monteiro, S.N. Production of Synthetic Ornamental Marble as a Marble Waste Added Polyester Composite. *Mater. Sci. Forum* **2014**, *775–776*, 341–345. [CrossRef]
35. Carvalho, E.A.S.; Marques, V.R.; Rodrigues, R.J.S.; Ribeiro, C.E.G.; Monteiro, S.N.; Vieira, C.M.F. Development of Epoxy Matrix Artificial Stone Incorporated with Sintering Residue from Steelmaking Industry. *Mater. Res.* **2015**, *18*, 235–239. [CrossRef]
36. *ABNT NBR15845-2*; Pedras Para Revestimento. Parte 2: Determinação da Densidade Aparente, Porosidade Aparente e Absorção de Água. Associação Brasileira de Normas Técnicas: Rio de Janeiro, Brazil, 2015.
37. *ABNT NBR15845-6*; Pedras Para Revestimento. Parte 6. Determinação do Módulo de Ruptura (Flexão de Três Pontos). Associação Brasileira de Normas Técnicas: Rio de Janeiro, Brazil, 2015.
38. *ABNT NBR 15845-5*; Rochas Para revestimento Parte 5: Determinação da Resistência à Compressão Uniaxial. Associação Brasileira de Normas Técnicas: Rio de Janeiro, Brazil, 2015.
39. *ABNT NBR 16596*; Rochas Para Revestimento—Resistência ao Ataque Químico—Método de Ensaio. Associação Brasileira de Normas Técnicas: Rio de Janeiro, Brazil, 2017.
40. *ABNT NBR 15845-3*; Rochas Para Revestimento Parte 3: Determinação do Coeficiente de Dilatação Térmica Linear. Associação Brasileira de Normas Técnicas: Rio de Janeiro, Brazil, 2015.
41. de Castro, V.G. Cimento Portland. In *Compósitos Madeira-Cimento: Um Produto Sustentável Para o Futuro*; EdUFERSA: Mossoró, Brazil, 2021; pp. 13–21. Available online: https://books.scielo.org/id/8skrw/pdf/castro-9786587108612-02.pdf (accessed on 13 October 2023).
42. Barreto, G.N.S.; Carvalho, E.A.S.; Souza, V.d.S.d.; Gomes, M.L.P.M.; de Azevedo, A.R.G.; Monteiro, S.N.; Vieira, C.M.F. Engineered Stone Produced with Glass Packaging Waste, Quartz Powder, and Epoxy Resin. *Sustainability* **2022**, *14*, 7227. [CrossRef]
43. Panzera, T.H.; Sabariz, A.L.R.; Strecker, K.; Borges, P.H.R.; Vasconcelos, D.C.L.; Wasconcelos, W.L. Mechanical properties of composite materials based on Portland cement and epoxy resin. *Cerâmica* **2010**, *56*, 77–82. [CrossRef]
44. Ribeiro, C.E.G.; Rodriguez, R.J.S.; Vieira, C.M.F. Production of Ornamental Compound Marble with Marble Waste and Unsaturated Polyester. In Proceedings of the TMS Annual Meeting, San Diego, CA, USA, 16–20 February 2014; pp. 129–136.
45. Peixoto, J.; Carvalho, E.A.S.; Gomes, M.L.P.M.; Guimarães, R.d.S.; Monteiro, S.N.; de Azevedo, A.R.G.; Vieira, C.M.F. Incorporation of Industrial Glass Waste into Polymeric Resin to Develop Artificial Stones for Civil Construction. *Arab. J. Sci. Eng.* **2022**, *47*, 4313–4322. [CrossRef]
46. *ASTM C503/C503M*; Standard Specification for Marble Dimension Stone. ASTM International: West Conshohocken, PA, USA, 2015.
47. Chiodi Filho, R. *Guia de Aplicação de Rochas em Revestimentos*; Abirochas: São Paulo, Brasil, 2009; Available online: www.abirochas.com.br (accessed on 13 October 2023).

48. Agrizzi, C.P.; Carvalho, E.A.S.; Gadioli, M.C.B.; Barreto, G.N.S.; de Azevedo, A.R.G.; Monteiro, S.N.; Vieira, C.M.F. Comparison between Synthetic and Biodegradable Polymer Matrices on the Development of Quartzite Waste-Based Artificial Stone. *Sustainability* **2022**, *14*, 6388. [CrossRef]
49. de Castro, A.L.; Pandolfelli, V.C. Revisão: Conceitos de dispersão e empacotamento de partículas para a produção de concretos especiais aplicados na construção civil. *Cerâmica* **2009**, *55*, 18–32. [CrossRef]
50. Debnath, S.; Ranade, R.; Wunder, S.; Mccool, J.; Boberick, K.; Baran, G. Interface effects on mechanical properties of particle-reinforced composites. *Dent. Mater.* **2004**, *20*, 677–686. [CrossRef] [PubMed]
51. silaex.com.br. Poliéster Insaturados. 2023. Available online: http://www.silaex.com.br (accessed on 4 November 2023).
52. do Amaral, T.D.; Taveira, S.F.; de Souza, T.P.; Noriega, C.L. Comparativo das metodologias da produção de ácido lático a partir do melaço de cana-de-açúcar e sua aplicação como biopolímero (PLA). *Rev. Científica Multidiscip. Núcleo Conhecimento* **2022**, 150–193. [CrossRef]
53. Carvalho, E.A.S.; de Souza, V.d.S.; Barreto, G.N.S.; Monteiro, S.N.; Rodriguez, R.J.S.; Vieira, C.M.F. Incorporation of Porcelain Powder and Mineral Wastes in Epoxy Matrix for Artificial Stone Purchase. In *Characterization of Minerals, Metals, and Materials*; Springer: Berlin/Heidelberg, Germany, 2021; pp. 435–443.
54. Silva, F.S.; Ribeiro, C.E.G.; Rodriguez, R.J.S. Physical and Mechanical Characterization of Artificial Stone with Marble Calcite Waste and Epoxy Resin. *Mater. Res.* **2017**, *21*, e20160377. [CrossRef]
55. RMC. Revestimento de Mármores Compactos S.A. 2022. Available online: https://www.rmc.pt/ (accessed on 8 January 2024).
56. Carvalho, E.A.S.; Vilela, N.d.F.; Monteiro, S.N.; Vieira, C.M.F.; da Silva, L.C. Novel Artificial Ornamental Stone Developed with Quarry Waste in Epoxy Composite. *Mater. Res.* **2018**, *21*, e20171104. [CrossRef]
57. Peng, L.; Qin, S. Mechanical behaviour and microstructure of an artificial stone slab prepared using a SiO2 waste crucible and quartz sand. *Constr. Build. Mater.* **2018**, *171*, 273–280. [CrossRef]
58. Gomes, M.L.P.; Carvalho, E.A.; Sobrinho, L.N.; Monteiro, S.N.; Rodriguez, R.J.; Vieira, C.M.F. Production and characterization of a novel artificial stone using brick residue and quarry dust in epoxy matrix. *J. Mater. Res. Technol.* **2018**, *7*, 492–498. [CrossRef]
59. Leal Da Cruz Silva, T.; Santos Carvalho, E.A.; Sales Barreto, G.N.; Perim da Silva, T.B.; João da Cunha Demartini, T.; Fontes Vieira, C.M. Characterization of artificial stone developed with granite waste and glass waste in epoxy matrix. *J. Mater. Res. Technol.* **2023**, *26*, 2528–2538. [CrossRef]

Disclaimer/Publisher's Note: The statements, opinions and data contained in all publications are solely those of the individual author(s) and contributor(s) and not of MDPI and/or the editor(s). MDPI and/or the editor(s) disclaim responsibility for any injury to people or property resulting from any ideas, methods, instructions or products referred to in the content.